

Design and validation of a lightweight adaptive and compliant locking mechanism for an ankle prosthesis

François Heremans¹, Bruno Dehez¹ and Renaud Ronsse¹

Abstract—Over the last decade, active lower-limb prostheses demonstrated their ability to restore a physiological gait for transfemoral amputees by supplying the required positive energy balance during daily life locomotion activities. However, the added-value of such devices is significantly impacted by their limited energetic autonomy and excessive weight preventing their full appropriation by the patients. There is thus a strong incentive to reduce both the overall power consumption and weight of active prostheses. To address these issues, we developed a novel parallel spring mechanism, tailored to the dynamical behavior of an ankle prosthesis. The first contribution is the development of a lightweight and adaptive locking system, comprising an energy efficient ratchet and pawl mechanism with electromagnetical actuation. As second contribution, the required compliance is directly materialized within the structure of the prosthesis with no additional parts, taking advantage of fused filament fabrication (FDM) technology with carbon fibers reinforcement. Our system provides an elastic torque during flat ground walking, corresponding to 41% of the peak torque produced by an healthy ankle (50 Nm), at a negligible energetic cost (0.5 J/stride). By design, the novel parallel spring mechanism is lightweight (140 g), can engage at any plantarflexion position with a locking discretization of 0.3°, and is self-unlocking.

I. INTRODUCTION

The past decade has seen a lot of research seeking to improve the locomotion capabilities of lower-limb amputees, by providing devices replacing their missing limb and being safe, energy-efficient, and intuitive to use [1]–[5]. A related expected impact of these research efforts is to increase the use of lower-limb prostheses by dysvascular amputees, representing 70% of all lower-limb amputees [6]. These strongly disabled patients face tremendous difficulties to use classical prostheses owing to the challenges associated to (i) providing more energy with the remaining joints [7], (ii) ensuring the overall body stability, and (iii) managing the cognitive effort which is required to walk with a prosthesis, mainly if it is passive [8]. In addition to these functional objectives, the design of a prosthesis must be guided by several other important criteria: safety, weight, encumbrance, energetic autonomy, comfort and cosmesis, including noise and appearance. Prosthesis design is also highly constrained by the stump/prosthesis connexion. Although progress has been made recently towards osseo-integration [9], a socket fixed to the stump using vacuum still remains the most

usual solution for achieving the human-prosthesis physical anchoring. As consequence, stump soft tissues have to cope with large pressures associated with weight bearing and dynamical transfer of propulsive forces. Furthermore, the swing motion of the leg can lead to uncomfortable inertial efforts due to the non-negligible mass of the prosthesis. This problem is even more critical for transfemoral amputees with a short stump, and critically limit the device usability for an extended period of time. The comfortable weight limit highly depends on the stump length, location and the activity level of the patient. Anyway, there are thus strong incentives for minimizing the weight of lower-limb prostheses.

These prostheses can be divided into passive and active devices. Only active ankle prostheses can provide the net positive energy being required during flat ground walking, and more complex tasks such as slope and stair ascend. This was recently demonstrated in [1], where the authors proved to normalize the gait pattern of transtibial amputees, both regarding kinematics and metabolic cost, using an active device. However, actuated systems tend to be bulkier and heavier than their passive counterparts. In an effort to reduce weight and encumbrance, existing devices embed series elastic actuators (SEA), this principle being reviewed in [10]. If correctly tuned, SEA might have a direct effect in decreasing the motor speed and thus further decrease the required peak electrical power. In sum, this offers to equip the prosthesis with smaller motors than those necessary for providing the whole peak power.

Yet, active prostheses are facing another big challenge, namely energetic autonomy. In order to maximize the efficiency, the actuator torque profile should also be minimized. Indeed, the motor torque is proportional to its current, and the motor Joule losses are proportional to the square of this current. Consequently, the RMS torque directly influences the motor dimensioning, and thus its cost, weight, and potential hazard for the user. Targeting this torque reduction, a common solution within lower-limb prostheses is to embed a parallel spring, passively generating torque on top of the SEA. Consequently, the actuator produces only the remaining fraction of the whole requested joint torque. As detailed in Section II, ideally, the parallel element should be unidirectional and should engage only above a certain joint angle, so that no torque is produced below that angle and torque ramps up above this threshold. In existing ankle prostheses, this parallel compliant element is implemented in two different ways, depending on the joint angle where torque production is triggered. The first type engages at a fixed joint angle, that is carefully chosen to be outside the range of motion of the

*This work was supported by the Belgian F.R.S.-FNRS (Aspirant #6809010 awarded to FH) and the Louvain Foundation.

¹ Mechatronic, Electrical Energy, and Dynamic Systems (MEED), Institute of Mechanics, Materials and Civil Engineering (iMMC), Institute of Neuroscience (IONS) and Louvain Bionics, Université catholique de Louvain, Belgium.

swing phase, see e.g. [1]. This type can only produce a torque boost in late stance. The second type can dynamically change the angle of engagement. This requires a clutch mechanism to anchor the spring when needed. Engaging early in the stance phase allows to store more elastic energy but requires the parallel spring to be deactivated somehow during the swing phase. Such adaptive parallel springs heavily rely on appropriate locking mechanisms, most having been reviewed in [11].

As mentioned above, global weight is another critical issue for a prosthesis. To the best of our knowledge, there is currently no propulsive bionic feet as light as their biological counterpart (foot and calf respectively 1.35% and 4.20% of body weight, i.e. 1.0 kg and 3.2 kg for a 75 kg individual [12]).

Building upon previous simulation results [13], the present work focuses on the development of a lightweight active ankle prosthesis. More precisely, this paper validates a novel adaptive parallel spring with an ultra low power locking mechanism. The proposed design takes advantage of fibers reinforced fused deposition modeling (FDM), leading to a design that both is lightweight and achieves high mechanical performances.

The paper is structured as follows. Section II briefly introduces the biological data guiding the development and dimensioning of an adaptive locking mechanism. Based on such data, Section III describes the proposed new electromechanical design. Experimental results are reported in Section IV, and the paper ends with a discussion and conclusion.

II. GAIT ANALYSIS

Biomechanical walking data such as those reported in [14] provides useful guidelines for the design of a propulsive bionic feet. In the sagittal plane, these data reveal that the ankle produces an unidirectional effort gradually increasing during the stance phase, and ending with a high power push-off, as shown in Fig. 1 (left). During normal walking, the peak torque/power of this joint are thus very high, i.e. about 120 Nm and 270 W for a 75 kg individual. Moreover, the torque vs. position curve of the joint follows drastically different pathways in the stance and swing phases, respectively. The stance phase is characterized by a non-linear torque ramp with a net energy production (16 J per stride) while the swing phase corresponds to joint motion with negligible effort, i.e. flat curve. Consequently, a unidirectional parallel spring with two alternating stiffnesses (high and zero stiffness) could fairly capture this torque/position profile, although it would lack the net energy production. Coupling this adaptive parallel spring to a SEA could thus reproduce the whole trajectory with minimum motor torque.

As demonstrated in our previous work [13], the engaging angle of such a parallel spring is critical, see Fig. 2. Prostheses embedding such a spring usually engage above a fixed angular threshold in order to not impede with the joint motion during the swing phase, see e.g. [1]. However, the consequence is that the spring only provides a reduced fraction of the total elastic response. Moreover, the prosthesis

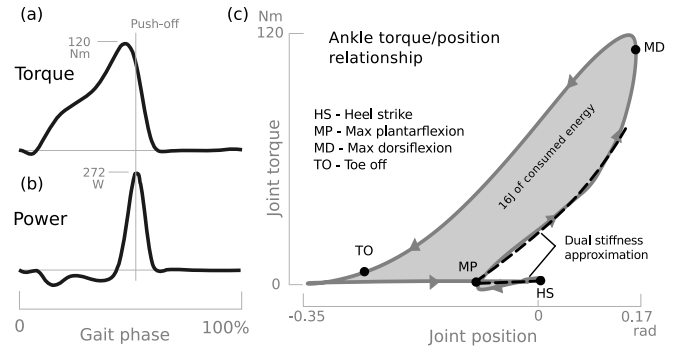


Fig. 1. Biomechanical data of the ankle joint for a 75 kg subject. (a) The joint displays a steadily increasing torque trajectory peaking at around 120 Nm just before push-off. (b) The peak power is around 270 W corresponding to the fast push-off motion. (c) Torque vs. position characteristic: the trajectory can be approximated by two parallel springs with different stiffnesses. The joint actively produces about 16 J. (Data adapted from [14]).

cannot adapt to different terrains, e.g. slopes, where the ideal joint kinematic would differ. In order to take advantage of the full elastic response of the joint, the parallel spring should engage at the maximum plantarflexion angle following heel strike (time t_a in Fig. 2) during the stance phase [5]. Moreover, the engagement should be prevented during the swing phase (time t_c in Fig. 2), so that no undesirable torque is generated during this phase. In the next section, we report a lightweight electro-mechanical system fulfilling these requirements.

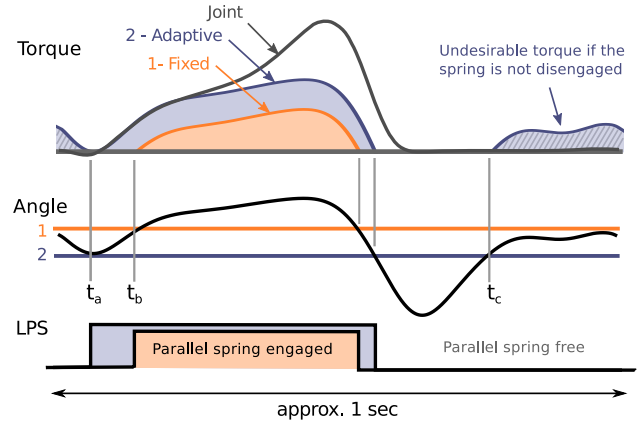


Fig. 2. A lockable parallel spring (LPS) with early engagement (2, blue) in t_a provides more torque than a fixed spring engaging later (1, orange) in t_b but requires to be disengaged before the swing phase in t_c .

III. DESIGN OF A NEW PARALLEL SPRING MECHANISM

The proposed design includes a compliant structure, a controlled lockable anchor and an aramid rope circuit, as depicted in Fig. 3. The controlled locking system provides anchorage for the rope system. Secondly, the structure of the prosthesis is FDM printed with carbon fibers reinforcement providing the required parallel elasticity, and thus removing the need for an external steel spring.

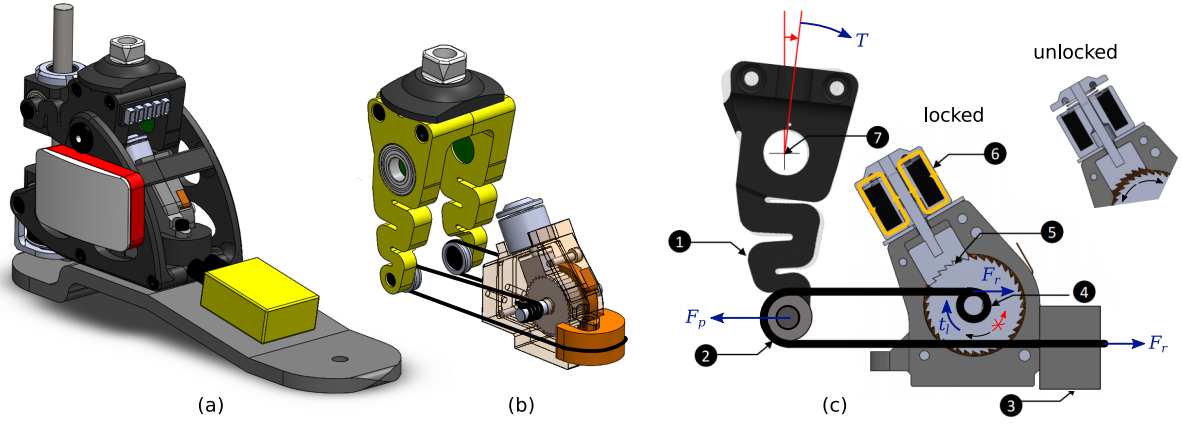


Fig. 3. Details of the locking mechanism; (a) Complete prosthesis CAD overview, (b) Isolated and exploded CAD view of the parallel spring and locking mechanism, (c) Functional description with internal details: (1) compliant lever arm, (2) pulley and aramid rope, (3) fixed anchor, (4) shaft preloaded with constant force spring, (5) ratchet and pawl mechanism, (6) spring loaded electro-magnet, (7) joint axis of rotation. In panel (c), efforts are denoted as: T the joint elastic torque, F_r the rope tension, F_p the pulley force and t_l the locking torque.

A. Locking mechanism

The system is symmetric and is composed of two compliant levers of length $l_c = 5$ cm (1) rotating around the prosthesis main revolute joint (7). The extremity of each lever is connected to a pulley (2), being itself part of a hoist made up with a high rigidity aramid rope. One part of the rope runs around a fixed block (3) and provides the primary anchorage. Furthermore, the rope is allowed to slide in order to equalize the force in both compliant arms. The other side of the rope is wound around a shaft of diameter $d_l = 6$ mm (4). The hoist reduces the force on the locking shaft (4) to half of the total force applied to the pulley (2), therefore providing a first 1:2 reduction stage. The shaft (4) is linked to a ratchet mechanism with 36 teeth (5). The pawl itself comprises 6 teeth providing the locker with high strength and a high locking resolution. The pawl block moves linearly to (un)lock the system.

The locking motion is generated by a small spring-loaded electromagnet with coil resistance of 50Ω , such that the system is unlocked if unpowered. The geometry of the teeth also make it self-locking. As soon as the ratchet and pawls get in contact with each other and the system is loaded, the electromagnet can be switched off while the system will remain locked (see Fig. 4). The morphology of the teeth prevents any unlocking under load and allows rotation of the axle in one direction even in the locked position. Therefore, locking does not have to be triggered with very accurate timing. Indeed, the locker can safely be energized at the beginning of the stance phase with the mechanism effectively engaging at the maximum plantarflexion angle. Furthermore, self-unlocking will occur when both the locking mechanism is powered off, and the load is removed. The stroke required for locking is very short (equal to the teeth height), allowing very fast locking, i.e. in about 30 ms. The control electronics only requires a power switch and a digital controller.

The shaft (4) is preloaded with a soft spiral spring tightening the rope at all time with constant force. The small

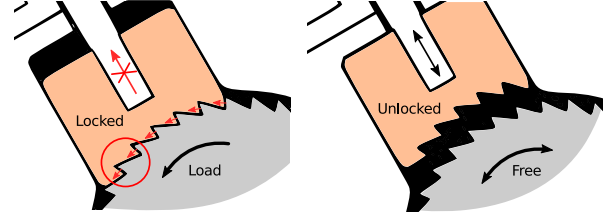


Fig. 4. Detail of the non-symmetric teeth profile achieving the self-locking property under load. Unlocking requires no power and is automatic when the loading force direction reverses.

diameter of the shaft induces a second and larger reduction stage, such that the total locking torque perceived at the locking mechanism t_l is 33 times smaller than the joint torque, i.e. 2.4 Nm for a 80 Nm joint torque T . This has a significant impact for the size and weight of the whole mechanism. In order to secure the rope on the axle, it is wound around it and terminated with a knot passing through the axle. By doing so, we take advantage of the capstan law [15], i.e. an exponential relationship exists between the holding force and the number of turns being wound. The small force required at the extremity of the knot F_k can be computed as a function of the minimum number of turns around the axle n (worst case scenario when the rope is maximally unwound) and the maximum rope tension F_r in each arm of the system, i.e:

$$F_r = \frac{T}{l_c \cdot 2 \cdot 2} \quad ; \quad F_k = \frac{F_r}{e^{\mu\phi}} \quad ; \quad \phi = 2\pi n$$

By taking $\mu = 0.4$ (i.e. the friction coefficient between aluminum and aramid [16], $n = 3$, and a joint torque $T = 80$ Nm, we obtain $F_r = 400$ N and $F_k = 0.2$ N, i.e. a very low holding force as compared to the one being sustained in the rope.

Furthermore, due to the fact that the number of teeth is finite, locking cannot happen everywhere and the mechanism experiences some locking backlash that can be quantified.

On the locker axle, the backlash θ_p is directly linked to the number of teeth $n_t = 36$, i.e.:

$$\theta_p = 360^\circ / n_t = 10^\circ$$

The rope moves by l_{rp} corresponding to this angular backlash:

$$l_{rp} = \theta_p \cdot d_l / 2 = 0.5 \text{ mm}$$

Due to the hoist system, the pulley displacement l_{pp} is half of the rope displacement at the shaft, i.e. $l_{pp} = l_{rp} / 2$. Finally, the backlash seen at the joint side θ_{pj} , is computed using the length of the compliant lever l_c , i.e.:

$$\theta_{pj} = l_{pp} / l_c = 0.3^\circ \text{ (0.005 rad)}$$

This joint backlash will thus likely have a negligible impact on the device behavior.

B. FDM printed elasticity

Instead of embedding dedicated springs in the mechanism transmission to render the desired parallel compliance, our design embeds it in the structural parts of the prosthesis itself. This brings a drastic decrease of in the number of parts, weight and complexity, although this requires to accurately engineer the parts to match the desired stiffness. Indeed, obtaining both large stresses and strains is challenging. To cope with this challenge, we explored the use of FDM printed continuous carbon fibers reinforced materials [17]–[19]. This provides the designer with a lot of freedom regarding the parts morphology while leveraging the continuous carbon fibers with high tensile strength (700 MPa) and modulus (54 GPa). The material is thus a composite of a low density nylon matrix and continuous carbon fibers. The fibers and core are arranged in a sandwich configuration minimizing the weight. Another interesting aspect of the polymer core is its natural damping dynamics. It has been shown that some series damping can add substantial benefits to force control performance and stability [20].

The stiffness of such sandwich parts (nylon core + carbon fibers shell) can be estimated using a simplified material model [21]. As depicted in Fig. 5, b , t , c , d are the geometric parameters of a general sandwich material.

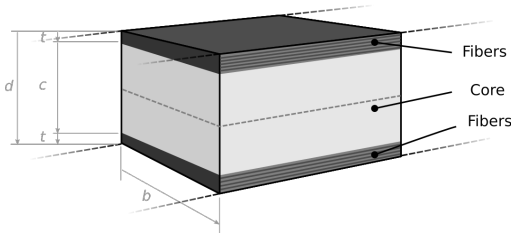


Fig. 5. Geometric parameters of a section of sandwich material: t - fiber layer height, c - core layer height, b - beam width, d - total height.

The flexural rigidity $(EI)_{eq}$ and the equivalent shear rigidity $(AG)_{eq}$ of the part can be computed using the core and shell material properties. E_c and G_c are the elastic and

shear modulus of the core, while E_f is the elastic modulus of the shell fibers:

$$(EI)_{eq} = \frac{E_f b t c^2}{2} ; \quad (AG)_{eq} = \frac{G_c b d^2}{c}$$

The core has a honeycomb or triangular structure such that its material properties E_c , G_c can be estimated using its density ρ_c and the properties of the bulk material (nylon) (E_s , ρ_s) [21]:

$$E_c = E_s \left(\frac{\rho_c}{\rho_s} \right)^2 ; \quad G_c = 0.4 \cdot E_s \left(\frac{\rho_c}{\rho_s} \right)^2$$

Using these equivalent materials properties, finite elements analyses [22] can be performed to provide a good estimate of the material behavior under load with complex geometries.

Fig. 6 shows a slice of the composite compliant lever used as parallel elasticity and combined to our locking mechanism. The continuous carbon fibers (shell) can be seen embedded in the nylon triangular matrix (core).

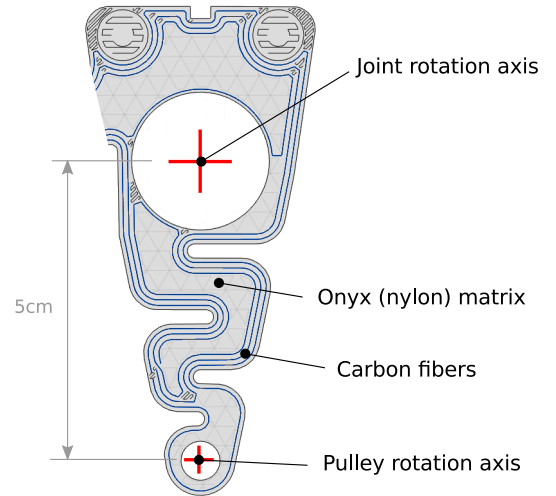


Fig. 6. Slice of the compliant lever embedding continuous fibers in the triangular nylon matrix. (Extracted from Markforged Eiger software).

C. Prototyping

The actual prosthesis and embedded parallel spring mechanism are depicted in Fig. 7. It was manufactured essentially by FDM printing with a few parts machined out of aluminum. The pylon and pyramid adapter were kindly provided by TruLife Prosthetics, Sheffield (UK).

IV. EXPERIMENTAL VALIDATION

In order to test the locking mechanism and future prostheses, a test bench was designed. This includes a single 220 W motor (Nanotec DB87S01), 40:1 gearbox (Apex Dynamics PEII090-040), 2:1 belt drive and a custom built torque sensor. The joint position is measured by a hall effect sensor AS5048 (accuracy 0.02°). The bench can actuate the prosthesis to emulate joint trajectories of daily life activities. The full bench is depicted in Fig. 8.

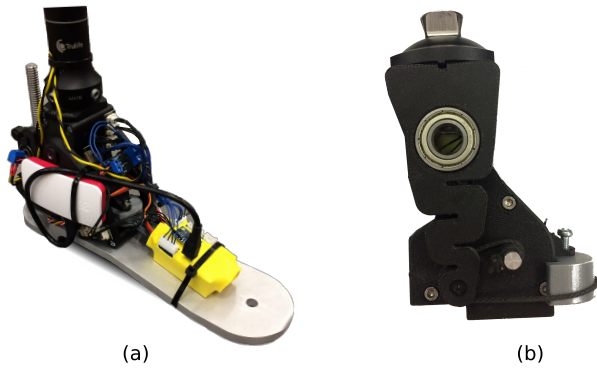


Fig. 7. Ankle prosthesis prototype embedding the locking mechanism, (a) full prototype, (b) locking mechanism.

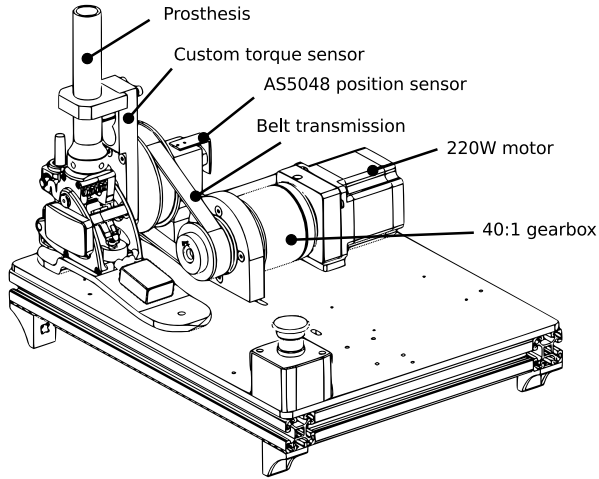


Fig. 8. Test bench for the prosthesis including a servo motor and a custom torque sensor.

A. Protocol

In order to measure the stiffness of the mechanism, the prosthesis was only connected to the designed locking mechanism through its parallel spring and its joint was position driven by the bench to follow a sinusoidal trajectory between -0.1 rad and 0.2 rad (corresponding to a simplified stance pattern, see Fig. 1). Locking was activated slightly before this position reaches its minimum by sending a 20 V, 30 ms pulse to the electromagnet (see Fig. 9). As soon as the velocity became positive, the locking mechanism actually engaged. The bench then measured the reaction torque along the trajectory. When reaching back the initial locking position, the locker automatically disengaged and the bench performed another cycle with no load. This procedure was performed three times. Computing the slope of the filtered and averaged position vs. torque curve gives an image of the equivalent stiffness of the parallel spring.

B. Results

Fig. 10 shows the torque vs. position characteristic of the parallel spring mechanism compared to a typical flat ground walking characteristics. It is observable that the mechanism

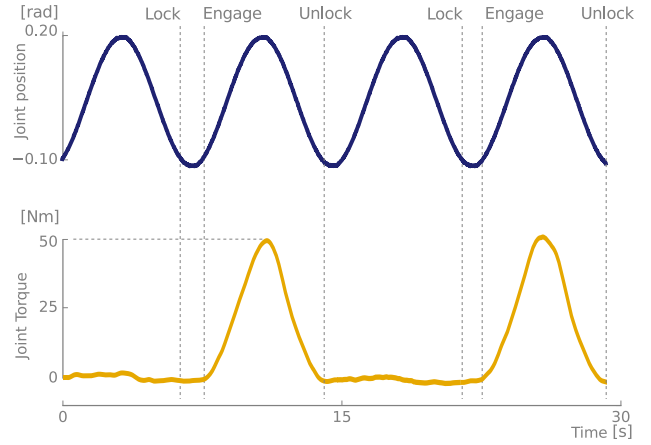


Fig. 9. Test trajectory: the joint is position driven to follow a sinusoidal trajectory (top) while the joint torque produced by the lockable parallel spring is measured (bottom).

exhibits the required biphasic torque characteristic, although the tested structure is slightly too compliant and only generates 50 Nm, i.e. 62% of the target 80 Nm required at push-off. The same figure shows the ideal characteristic that is aimed to be obtained with the next version of the parallel spring. Regarding the locking actuation, the device is only powered with a 20 V burst lasting 30 ms to quickly close the magnetic circuit. This corresponds to 0.50 J of energy per stride, thus about 3% of the energy required by one ankle stride (16 J/stride). The system then remains locked as long as a load is applied (no power consumption) and automatically unlocks itself when the load vanishes. The weight of the locking system alone is 140 g.

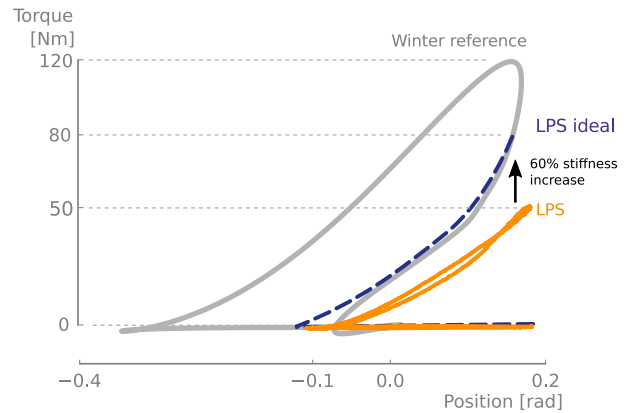


Fig. 10. Torque vs. position relationship of the lockable parallel spring (LPS) averaged over multiple cycles compared to the ideal characteristics and Winter data [14]. The flat region corresponds to cycles where the locking system was purposely not activated.

V. DISCUSSION & PERSPECTIVES

The proposed ankle compliant locking device exhibited interesting characteristics but also opened new challenges.

A. Compliant structure

The compliant element features a slightly too low stiffness. This was somehow expected since we used a simplified model to predict the material behavior with FEA. Further tuning of the material model should lead to better matching, although the design phase of such a mechanism should always consist in iterating between simplified FEA modeling and experimental validation. The pace between these iterations are typically constrained by manufacturing constraints, non-linear behavior of the composite structure, and modeling complexity. Moreover, the whole prosthesis also deforms under load, further limiting the maximum achievable stiffness.

At a latter stage, a good stiffness predictor could offer to adapt the compliant element stiffness for every subject by printing a new part matching his/her morphology. Furthermore, topology optimization might even be conducted in order to further decrease the component's weight.

B. Locking mechanism

The high reduction ratio in the system offered to design a small and lightweight locker. Also, by including a powerful parallel locking system, the requirements on any active module were also greatly reduced. This should lead to the design of an active prosthesis having a global smaller weight than existing devices. Furthermore, the ability to lock in every position is desirable for adapting to uneven and non-flat terrains that are ubiquitously encountered during daily life activities.

C. Future developments

Future works include the tuning of the elastic structure to match the required stiffness. Also, the experimental validation of a series elastic actuator working on a similar compliance principle and going in parallel to this locker will be explored. This will enable power delivering and dissipation. Finally, clinical tests will be conducted with amputees wearing the device, and its performance will be compared to existing devices.

VI. CONCLUSION

This paper described a new design providing an original solution to well-known issues regarding energetic consumption and weight of current active ankle prostheses. This solution relied on the design of a lockable parallel spring that can engage early in the stance phase and passively provide most of the torque required during flat ground walking. This would greatly reduce the torque requirements on the active module and improve its efficiency. The proposed system includes a lightweight unidirectional clutch with a compliant element, being embedded directly in the structure of the prosthesis (140 g). This is achieved through the use of advanced FDM printing, embedding carbon fibers inside a nylon matrix. Our system was experimentally validated. The torque vs. position characteristic of the system is promising, although stiffness should be increased by 60% in order to reach typical flat ground walking specifications. The energy consumed during locking is small, i.e. only 0.5 J/stride and the locking backlash is negligible (0.3°).

REFERENCES

- [1] H. M. Herr and A. M. Grabowski, "Bionic ankle-foot prosthesis normalizes walking gait for persons with leg amputation," *Proceedings. Biological Sciences / The Royal Society*, vol. 279, no. 1728, pp. 457–464, Feb. 2012.
- [2] R. D. Bellman, M. A. Holgate, and T. G. Sugar, "SPARKy 3: Design of an active robotic ankle prosthesis with two actuated degrees of freedom using regenerative kinetics." IEEE, 2008, pp. 511–516.
- [3] J. Geeroms, L. Flynn, R. Jimenez-Fabian, B. Vanderborght, and D. Lefeber, "Ankle-knee prosthesis with powered ankle and energy transfer for cyberlegs α -prototype," in *Rehabilitation robotics (ICORR), 2013 IEEE int. conf. on.* IEEE, 2013, pp. 1–6.
- [4] B. E. Lawson, J. Mitchell, D. Truex, A. Shultz, E. Ledoux, and M. Goldfarb, "A Robotic Leg Prosthesis: Design, Control, and Implementation," *IEEE Robotics & Automation Magazine*, vol. 21, no. 4, pp. 70–81, Dec. 2014.
- [5] P. Chernelle, V. Grosu, M. Cestari, B. Vanderborght, and D. Lefeber, "The amp-foot 3, new generation propulsive prosthetic feet with explosive motion characteristics: design and validation," *BioMedical Engineering OnLine*, vol. 15, no. 3, p. 145, Dec 2016.
- [6] P. L. Ephraim, T. R. Dillingham, M. Sector, L. E. Pezzin, and E. J. MacKenzie, "Epidemiology of limb loss and congenital limb deficiency: a review of the literature1," *Archives of Physical Medicine and Rehabilitation*, vol. 84, no. 5, pp. 747–761, May 2003.
- [7] R. L. Waters and S. Mulroy, "The energy expenditure of normal and pathologic gait," *Gait & Posture*, vol. 9, no. 3, pp. 207–231, July 1999.
- [8] R. M. Williams, A. P. Turner, M. Orendurff, A. D. Segal, G. K. Klute, J. Pecoraro, and J. Czerniecki, "Does having a computerized prosthetic knee influence cognitive performance during amputee walking?" *Archives of Physical Medicine and Rehabilitation*, vol. 87, no. 7, pp. 989–994, July 2006.
- [9] J. S. Hebert, M. Rehani, and R. Stiegelmar, "Osseointegration for Lower-Limb Amputation: A Systematic Review of Clinical Outcomes," *JBJS Reviews*, vol. 5, no. 10, p. e10, Oct. 2017.
- [10] K. Junius, P. Chernelle, B. Brackx, J. Geeroms, T. Schepers, B. Vanderborght, and D. Lefeber, "On the use of adaptable compliant actuators in prosthetics, rehabilitation and assistive robotics," in *ResearchGate*, July 2013, pp. 1–6.
- [11] M. Plooiij, G. Mathijssen, P. Chernelle, D. Lefeber, and B. Vanderborght, "Lock your robot: A review of locking devices in robotics," *IEEE Robotics Automation Magazine*, vol. 22, no. 1, pp. 106–117, 2015.
- [12] C. E. Clauser and al, "Weight, volume and center of mass of segments of the human body," *Air Force Systems Command*, 1969.
- [13] F. Heremans and R. Ronsse, "Design of an energy efficient transfemoral prosthesis using lockable parallel springs and electrical energy transfer," in *2017 International Conference on Rehabilitation Robotics (ICORR)*, July 2017, pp. 1305–1312.
- [14] D. A. Winter, *Biomechanics and Motor Control of Human Movement*. John Wiley & Sons, Oct. 2009, google-Books-ID: _bFHL081WfWc.
- [15] R. C. Juvinall and K. M. Marshek, *Fundamentals of machine component design*. Wiley New York, 2000, vol. 1.
- [16] M. Martinez, C. Navarro, R. Cortes, J. Rodriguez, and N. Sanchez-Galvez, "Friction and wear behaviour of kevlar fabrics," *Journal of materials science*, vol. 28, no. 5, pp. 1305–1311, 1993.
- [17] F. Ning, W. Cong, J. Qiu, J. Wei, and Y. Wang, "Additive manufacturing of carbon fiber reinforced thermoplastic composites using fused deposition modeling," *Composites Part B: Engineering*, vol. 80, pp. 369–378, Oct. 2015.
- [18] X. Wang, M. Jiang, Z. Zhou, J. Gou, and D. Hui, "3d printing of polymer matrix composites: A review and prospective," *Composites Part B: Engineering*, vol. 110, pp. 442–458, Feb. 2017.
- [19] R. Matsuzaki, M. Ueda, M. Namiki, T.-K. Jeong, H. Asahara, K. Horiguchi, T. Nakamura, A. Todoroki, and Y. Hirano, "Three-dimensional printing of continuous-fiber composites by in-nozzle impregnation," *Scientific Reports*, vol. 6, p. 23058, Mar. 2016.
- [20] A. Calanca, R. Muradore, and P. Fiorini, "A Review of Algorithms for Compliant Control of Stiff and Fixed-Compliance Robots," *IEEE/ASME Transactions on Mechatronics*, vol. 21, no. 2, pp. 613–624, Apr. 2016.
- [21] L. J. Gibson and M. F. Ashby, *Cellular Solids: Structure and Properties*, 2nd ed., ser. Cambridge Solid State Science Series. Cambridge University Press, 1997.
- [22] J. E. Akin, "SolidWorks Simulation Overview," in *Finite Element Analysis Concepts*. WORLD SCIENTIFIC, Aug. 2010, pp. 23–34, doi: 10.1142/9789814313025_0002.